Stability analysis of soilbag retaining wall under seismic loading

Eun Chul Shin[1], H.S. Shin[2], K.W. Park[3]

[1] Professor, Department of Civil Engineering, Incheon National University, 119 Academi-ro, Yeonsu-gu, 22012, Incheon,
[2] Ph.D, Department of Civil Engineering, Incheon National University, 119 Academi-ro, Yeonsu-gu, 22012, Incheon,
[3] Master, Department of Civil Engineering, Incheon National University, 119 Academi-ro, Yeonsu-gu, 22012, Incheon,

ABSTRACT

The earthquake that occurred in Korea until 2016 is mainly in the sea. Because of there is no damage to inland structures or human life, so the seriousness about earthquake is not well awared. However, the recent earthquakes in Pohang(2017, M=5.4) and the Gyeongju(2016, M=5.4) have caused anxiety among the people. Therefore, it is necessary to secure seismic stability not only for large structures, but also for infrastructure around living spaces in Korea. In this study, several large-scale shaking table tests on retaining wall of soilbag with flexible characteristic were conducted to investigate the structure integrity of soilbag retaining wall under the seismic loadings. Experimental conditions were set at 0.44g of the maximum ground acceleration with 2400 years recurrence interval. The ground acceleration for the shaking table test was in the range of 0.154g to 0.44g. Also, a finite element analysis with considering seismic loading was carried out by using the experimental results. As a result, considering the necessity of relatively lower height of retaining wall for the road-side and the mountainous area, and considering the surrounding environment factors, the soilbag retaining wall is very effective with considering eco-friendly environment and seismic stability.

Keywords: soilbag, retaining wall, earthquake, seismic wave, action point, dynamic earth pressure

1 INTRODUCTION

The earthquake that occurred in Korea until 2016 is mainly in the sea. Because of there is no damage to inland structures or human life, so the seriousness about earthquake is not well awared. However, the recent earthquakes in Pohang(2017, M=5.4) and the Gyeongju(2016, M=5.4) have caused anxiety among the people. And nowadays frequent aftershocks are continuing to realize the seriousness of the earthquake. In addition, since Korean people have little experience of earthquakes, education on evacuation and behavioral techniques has not done sufficiently.

Damage caused by an earthquake is not limited to physical property, but it also causes loss of life. As the damage to the people is caused by the structure or collapse around the living space, the seismic stability of the structure should be sufficiently secured. Therefore, the seismic stability must be secured not only for large structures but also for infrastructure around the living space. There is also a growing interest in seismic stability of retaining wall which are common infrastructures around us. Since the collapse of the retaining wall can cause injury, securing the earthquake stability is very important.

Many studies have been conducted on the behavior of retaining wall structures during earthquakes based on the Mononobe-Okabe's theory. This theory considers the inertia force of the backfill material in the static equilibrium state. However, most of them are about rigid retaining walls, most of them are 1 g scale shaking table experiments.

In this study, several large-scale shaking table tests on retaining wall of soilbag with flexible characteristic were conducted to investigate the structure integrity of soilbag retaining wall under the seismic loadings. Experimental conditions were set at 0.22g of the maximum ground acceleration with 2400 years recurrence interval. The ground acceleration for the shaking table test was in the range of 0.154g(0.22g×70%) to 0.44g(0.22g×200%). Also, a finite element analysis with considering seismic loading was carried out by using the experimental results.

2 THEORETICAL BACKGROUND

2.1 Earth pressure on retaining wall under seismic loading

Not only static earth pressure, but also dynamic earth pressure develops in retaining wall structures in an earthquake. Dynamic earth pressure as the lateral load additionally developed affects the stability of structure, and is affected by backfilling ground behavior, foundation ground, mine hoe flexibility, inertial force,

and seismic wave (Anderson et al., 2008; Yang et al., 2014; Yang et al., 2018).

Mononobe and Matsuo (1929) presented dynamic earth pressure theory, which is a modified version of Coulomb's sliding wedge analysis. Based on the idea that wall displacement is caused by vibration of the retaining wall in an earthquake, Richards and Elms (1979), Chang (1981), and Elms and Richards (1991) induced a dynamic earth pressure equation in which Dubrova (1963) assumption is applied.

Sherif et al. (1982) and Bolton and Steedman (1982) suggested that the Mononobe-Okabe method considering the conditions of static equilibrium state in 1-g shaking table test appropriately assessed dynamic earth pressure. Atik and Sitar (2010) determined the inertial force of mine hoe and phase difference between dynamic earth pressures and observed triangle distribution of earth pressure by conducting dynamic centrifugal model experiment and numerical analysis on U-shaped cantilever type retaining wall at 5.67 m height. This implies that the action point of dynamic earth pressure is near H/3, the same as the static earth pressure.

Meanwhile, Kim et al. (2003) and Yoon et al. (2005) conducted a 1-g_n shaking table test on the gravity quay wall and retaining wall, to analyze the effect of inertial force of structure on dynamic earth pressure. The test result showed that the actual dynamic earth pressure on the retaining wall was lower than the theoretical dynamic earth pressure, due to the phase difference between dynamic earth pressures in the mine hoe caused by inertial force of structure and backfilling material. The dynamic earth pressure calculated by the Mononobe-Okabe method was considered to be the upper limit.

Jung et al. (2010) proposed an elasticity theoretic equation to calculate the dynamic earth pressure of retaining wall, and argued that the dynamic earth pressure decreased with decreased flexibility, leading to low action point. According to the proposed elasticity theoretic equation, the Mononobe-Okabe method might underestimate dynamic earth pressure applied to the retaining wall.

A brief explanation of the theoretic equation to calculate dynamic earth pressure is as follows: Of the methods to calculate the retaining wall-applied dynamic earth pressure, the Mononobe theory is a modified version of the Coulomb theory, which is applicable to cohesionless soil. The dynamic active earth pressure and dynamic passive earth pressure upon earthquake can be expressed in Eqs. (1) ~ (5).

$$P_{AE} = K_{AE}(1-k_v)\frac{\gamma H^2}{2} \quad (1)$$

$$P_{PE} = K_{PE}(1-k_v)\frac{\gamma H^2}{2} \quad (2)$$

$$K_{AE} = \frac{sin^2(\alpha+\phi-\psi)}{sin^2\alpha\, cos\psi \sin(\alpha-\delta+\psi)\left[1\pm\sqrt{\frac{\sin(\phi-\delta)\sin(\phi-\psi-\beta)}{\sin(\alpha-\delta+\psi)\sin(\alpha+\beta)}}\right]^2} \quad (3)$$

$$K_{PE} = \frac{sin^2(\alpha-\phi-\psi)}{sin^2\alpha\, cos\psi \sin(\alpha+\delta+\psi)\left[1\pm\sqrt{\frac{\sin(\phi+\delta)\sin(\phi-\psi-\beta)}{\sin(\alpha+\delta+\psi)\sin(\alpha+\beta)}}\right]^2} \quad (4)$$

$$\psi = tan^{-1}\left(\frac{k_h}{1-k_v}\right) \quad (5)$$

where, P_E = dynamic earth pressure; β = tilt angle of backfilling banking; P_{AE} = dynamic active earth pressure; δ = friction angle of wall surface; P_{PE} = dynamic passive earth pressure; ϕ = internal friction angle of soil; and K_{AE} = coefficient of dynamic active earth pressure; and where k_h = coefficient of horizontal earthquake acceleration (=α_h/g_n); K_{PE} = coefficient of dynamic passive earth pressure; k_v = coefficient of vertical earthquake acceleration (α_v/g_n); γ = unit weight of soil; g_n = gravitational acceleration, H = height of wall; α_h = horizontal earthquake acceleration; α = tilt angle of rear wall; and α_v= vertical earthquake acceleration.

Seed-Whitman (1970) proposed Eq. (6) as a simple calculation for dry cohesionless soil with vertical wall and horizontal backfilling. The maximum dynamic active earth pressure (P_{AE}) is equivalent to the combined increments of the initial static and dynamic active earth pressure.

$$P_{AE} = P_A + \Delta P_{AE} = K_A\frac{\gamma H^2}{2} + \Delta P_{AE} \quad (6)$$

where, P_A refers to the initial static active earth pressure; ΔP_{AE} refers to increments of dynamic active earth pressure; and K_A refers to the coefficient of initial static active earth pressure. For increments of dynamic active earth pressure, the inertial force applied to the wedge at $\frac{3}{4}H$ distance from the peak of wall can be expressed by Eq. (7), and the action point of increments of dynamic active earth pressure (ΔP_{AE}) is applied to 0.6H from the bottom.

$$\Delta P_{AE} \backsimeq \left(\frac{3}{4}k_h\right)\frac{\gamma H^2}{2} \quad (7)$$

2.2 Stress characteristics on soilbag retaining wall

Fig. 1 shows the stress behavior of the soilbag. When an external force is applied to the soilbag, a tensile force(T) is generated, and due to the tensile force, additional restraint stress($\sigma_{01} = \frac{2t}{B}, \sigma_{03} = \frac{2T}{H}$) acts on the fill material of soilbag. Therefore, as shown in Fig. 1, principal stress is applied to a plane parallel to a major axis, and principal stress is applied to a plane parallel to a minor axis. Based on this principal stress, the stress can be expressed as Eq. (8) when the soilbag filler is shear

failure.

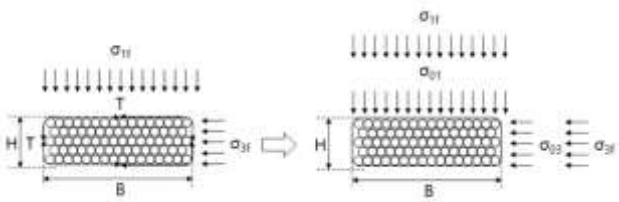

(a) stress of soilbag (b)stress of fill material

Fig. 1.Stress acting on soilbag and fill material

$$\sigma_{1f} + (2T/B) = K_p(\sigma_{3f} + (2T/H) \quad (8)$$

$$\sigma_{1f} = \sigma_{3f}K_p + (2T/B)\left[(B/H)K_p - 1\right] \quad (9)$$

Eq. (8) and Eq. (9) can be expressed by the relationship as shown in Eq. (10).

$$\sigma_{1f} = \sigma_{3f}K_p + 2c\sqrt{K_p} \quad (10)$$

Cohesion *c* can be summarized as Eq. (11).

$$c = (T/B)\left[(B/H)K_p - 1\right]\sqrt{K_p} \quad (11)$$

Therefore, the vertical load and the lateral load that are generated by using the soilbag are expressed as Equation (11) due to the restrained stresses generated in the soilbag, and they have stability against the external force.

2.3 Standard of seismic design in Korea

The seismic rating of the facility is classified as earthquake Ⅱ grade, earthquake Ⅰ grade, and earthquake sepcial grade according to the importance of facilities. The level of seismic performance is divided into the level of functional performance and the level of collapse prevention. Table 1 describes the seismic rating criteria according to the level of seismic performance.

Table 1. Seismic rating standard according to seismic performance level

Recurr-ence period \ Performance level	Performance of function	Preventing collapse
50yr	II	
100yr	I	
200yr	Special	
500yr		II
1000yr		I
2400yr		special

The design ground motion level is set as an earthquake zone separated from Gyeonggi Province and south of Gangwon Province based on the results of the earthquake disaster analysis. Zone coefficients Z in each seismic zone are tabulated in Table 2.

Table 2. Zone coefficient according to seismic zone

Seismic zone	Ⅰ	Ⅱ
Zone coefficient	011g	0.07g

Table 3 presents the maximum effective ground acceleration ratio(risk factor) by average recurrence period.

Table 3. Risk factor according to average seismic period

Seismic period (yr)	50	100	200	500	1000	2400
Risk factor	0.40	0.57	0.73	1.00	1.40	2.00

3 SHEAR STRENGTH OF THE SOILBAG

3.1 Experimental Method

The soilbag used in the construction of relatively low-height retaining walls in mountain areas, river banks, and roads is a system using the geotextile container construction method, which is constructed by installing the connecting materials between soilbags. The connecting materials used are the influential factor on the behavior of the soilbag system, which affect the friction between the soilbag and the surface of the framework member.

Fig. 2 shows a schematic of the large-scale direct shear test that was conducted to characterize the friction on the contact surface of the soilbag. The large-scale direct shear tester consists of upper box and lower box, of which the size is (300 mm × 300 mm × 200 mm) height. Vertical and horizontal displacements were measured by linear variable differential transformer (LVDT) installed at the action point of the vertical load and the lower part of the shear box. The displacement and shearing force values measured in the experiment are transferred via the data logger of the TDS-530 model in real time. In the experiment, horizontal displacement was controlled at 1 mm/min speed, and vertical stress intensity was controlled as being under (50, 100, and 150) kPa conditions, respectively.

The cohesion (c) and internal friction angle (ϕ) were obtained by pulling the soilbag-soil, soilbag-soilbag, and soilbag-connecting materials-soilbag inside the shear box, according to each experimental condition described in Fig. 3

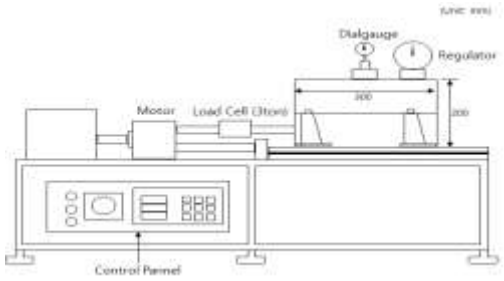

Fig. 2.Schematic of the large-scale Direct shear tester

(a) Soilbag-soil

(b) Soilbag-Soilbag

(c) Soilbag-Connecting materials-Soilbag

Fig. 3. Full View of the large-scale direct shear test

3.2 Experimental results of filling soil and soilbag

The filling material inside the soilbag was made of granite weathered soil, which can be easily collected around the site. Table 3 shows the physical properties of soil samples.

Items	Result
Natural water content (%)	18.5
Specific gravity (G_s)	2.68
Uniformity coefficient (C_u)	8.28
Curvature coefficient (C_c)	1.11
Maximum dry unit weight (kN/m^3)	18.8
Optimum water content (%)	11.3
U.S.C.S	SW

Fig. 4 shows the results of the direct shear test for various contact cases in the soilbag retaining wall system.

The shear strength between the soilbags was characterized as decreased cohesion between the soil and the bag with increased internal friction angle caused by the frictional angle of the soilbag. The shear strength between the soilbag–connecting material–soilbag was characterized as a slight increase in internal friction angle with increase in connection strength between the soilbag and the connecting materials, compared to the absence of connecting materials.

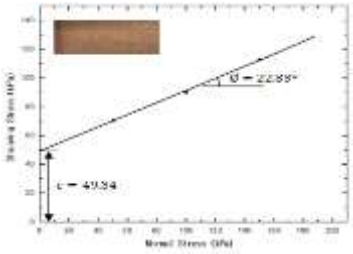

(a) Soilbag-Soil

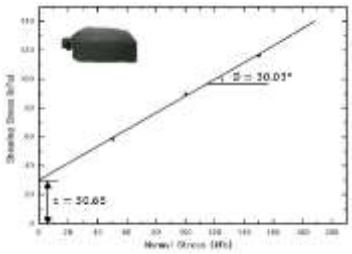

(b) Soilbag-Soilbag

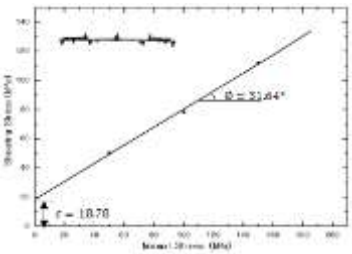

(c) Soilbag-Connecting materials-Soilbag

Fig. 4.Cohesion and internal friction angle by material

The friction angle and cohesion calculated from the large-scale direct shear test showed differences in the effect by the coefficient of friction. Collios et al. (1980) suggested Eq. (12) in friction on the interface between the soil and the geotextile, and determined the coefficient of friction. Fig. 5 shows the coefficient of friction for the result of each experiment.

$$e_{eff} = \frac{tan\delta}{tan\phi} \tag{12}$$

where, e_{eff} = coefficient of friction; $tan\delta$ = friction angle in the interface between the soil and the geotextile; and $tan\phi$ = friction angle in the interface between the soils.

4 LARGE-SCALE SHAKING TABLE TESTS

4.1 Overview of experiment

In the large-scale shaking table test conducted to assess earthquake resistance by using the 1-g_n shaking table, variables such as the slope of the soilbag system,

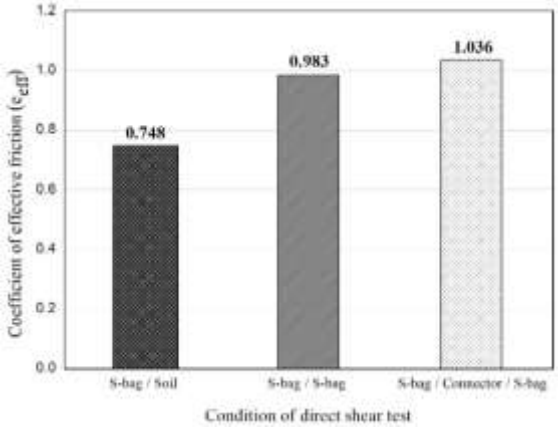

Fig. 5. Coefficient of friction with experimental conditions

the level of ground bed acceleration, and seismic wave were considered. Using the Hachinohe wave, which is a long period wave at relatively broad amplitude with high damage potential, the El-Centro wave, which is commonly used in earthquake resistance stability analysis, and the design basis response spectrum, the shaking table test was conducted in the increasing level of ground motions that created artificial seismic wave.

The level of ground motion was applied as 0.22 g_n by reflection Z value of the earthquake area coefficient as 0.11 and risk coefficient as 2.00 equivalent to that in 2,400 of recurrence period, according to the importance of social infrastructure. Based on 0.22 g_n of ground motion, the seismic wave input was increased by (70, 100, 150, and 200) %.

Taking into account the construction conditions in the target area where the soilbag retaining wall system will be applied, the maximum slope of retaining wall was set as 1:0.3, while the slope for connecting materials to be installed for construction of the soilbag system was set as 1:1. Fig. 6 shows the conditions of the shaking table test for the soilbag retaining system, where SB refers to Soil-Bag, and 0.3 and 1.0 refer to each slope.

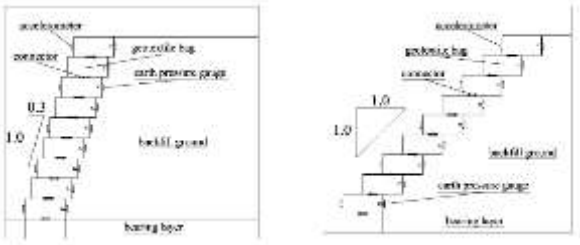

(a) SB1-0.3 (b) SB1-1.0

Fig. 6. Model Ground per Slope of Soil Bag

4.2 Experimental method

In general, the linear variable differential transformer (LVDT) is used to measure the displacement of structure at the static state of experimental conditions. However, it is difficult to install LVDT in the structure where dynamic load is imposed per a few hundredths, and accurate measurement is hardly conducted when LVDT is in direct contact with the structure. Therefore, in this experiment, displacement was rather precisely observed by using the non-contact video extensometer from IMETRUM. The maximum error produced by the non-contact video extensometer is 0.01 mm, and multi-focal monitoring can be conducted at a maximum 400 Hz. The range of measurement by the earth pressure gauge is 50 mm of diameter with maximum 200 kPa. The earth pressure gauge was installed horizontally on the rear of the retaining wall to measure the lateral earth pressure imposed on the contact surface between the soilbag and backfilling materials. Accelerations of the wall and the backfilling soil can be measured simultaneously using the accelerometer.

Fig. 7 shows how the soilbag can be laid in the soil box model at 1:0.3 (SB1-0.3) and 1:1 (SB1-1.0) of slope condition, respectively. Geomembrane was attached on the wall surface in order to minimize the friction force in the ground model and soil tank, as shown in Fig. 7 (a). This was a double structure, in which lubricant was applied between the geomembranes, and then the geomembrane or vinyl was attached again. Fig. 7 (b) shows that the soilbags were laid and compacted with compacting rod (4~5) times to secure > 90 % relative compaction, and then the bag thickness was measured. Fig. 7 (c) shows the full view of the horizontal and vertical earth pressure gauge to be installed on the rear of the soilbag. In order to level the earth pressure gauge, sand was laid at (1~2) cm thickness; the surface was made uniform by using the aligner; and the horizontality was checked. Fig. 7 (d) shows that the soilbag was laid up, and the soil of the rear retaining wall was backfilled and compacted. The dry unit weight was measured by using the sand cone method to determine the relative compaction of the soilbag and the rear surface, as described in Fig. 7 (e). Fig. 7 (f) is the full view of the beating point to be installed in each soilbag by using real time recording and displacement measurement by

optical camera, after the ground bed was built.

(a) Installation of geomembrane

(b) Determination of soilbag Thickness

(c) Installation of earth pressure gauge

(d) Laying-up of soilbag

(e) Density compaction test

(f) Accelerometer and displacement beating points

Fig. 7. Shaking table test set-up of soilbag retaining wall

Actual seismic records may not meet the design response spectrum even if they meet the target maximum by adjusting their size. Also, earthquakes that meet the design response spectrum are artificially generated and applied to the experiment because there is no actual recorded waveform. Fig. 8 shows the design response spectrum for artificial seismic waves. Artificial seismic waves are generated by using the program of EQ-maker, and Fig. 8 (c) shows artificial seismic waves.

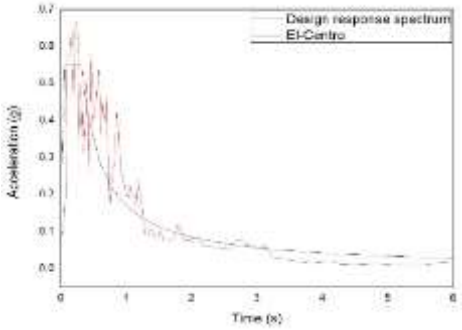

(a) El-Centro

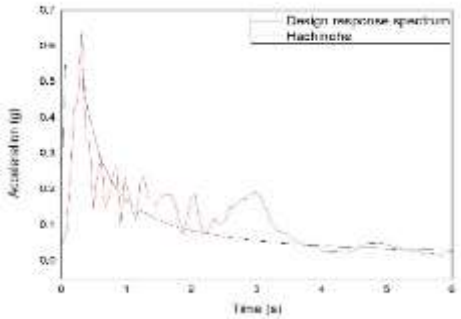

(a) Hachinohe

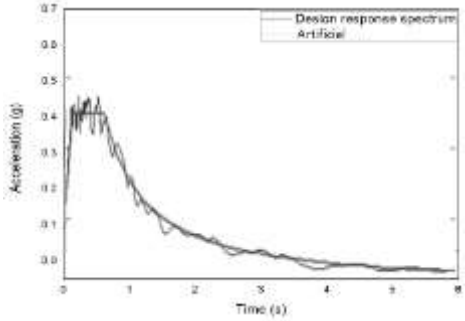

(c) Artificial

Fig. 8. Design Response Spectrum and Seismic Wave

4.3 Experimental results

4.1 Displacement

Fig. 9 shows the maximum displacement per height of the soilbag retaining wall that are imposed on the retaining wall at SB1-0.3 and SB1-1.9, respectively. Displacement of the soilbag retaining wall that occurs upon earthquake was analyzed under the classification as displacement in the direction of the facing retaining wall, displacement in the direction of the rear retaining wall, and final displacement after the end of experiment. The analysis results show that behaviors in the direction of the facing and rear retaining wall occurred in both cases of SB1-0.3 and SB1-1.0 where El-Centro, Hachinohe, and artificial seismic waves were applied. However, the displacement after the shaking table test shows ≤ 1 mm of elastic behavior, regardless of the slope of the retaining wall. This suggests that the connecting materials installed between the soilbags connect the bags like an integral system.

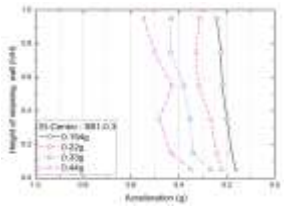

(a) El-Centro (SB1-0.3)

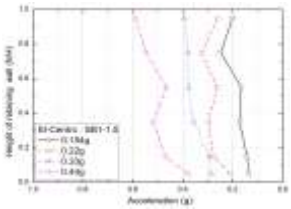

(d) El-Centro (SB1-1.0)

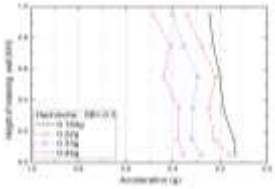
(b) Hachinohe (SB1-0.3)

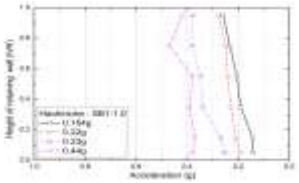
(e) Hachinohe (SB1-1.0)

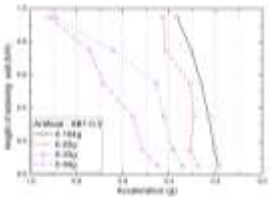
(c) Artificial (SB1-1.0)

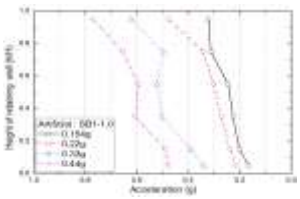
(f) Artificial (SB1-1.0)

Fig. 9. Maximum Displacement by height of soilbag retaining wall

4.2 Earth pressure

The lateral earth pressure applied to the rear surface of the soilbag retaining wall was estimated by various method for given two slopes, SB1-0.3 and SB1-1.0, respectively.

Fig. 10 shows that the lateral earth pressure by Jaky(1948) was calculated using the coefficient of static earth pressure at 30° of internal friction angle, and the lateral earth pressure by Coulomb(1776) was calculated at 0° of backfilling ground and frictional angle between the wall and the backfilling, equivalent to 2/3 of the internal friction angle.

The lateral earth pressure on the soilbag retaining wall reaches a peak at approximately 0.3H point from the bottom, regardless of the slope; and rapidly decreases as the height is lower than the 0.3 H point, suggesting the tendency of lateral earth pressure to gradually decrease as the height of the retaining wall becomes higher. At the 0.3 H point of the retaining wall, the lateral earth pressures at SB1-0.3 and SB1-1.0 were 6.94 and 6.39 kPa, respectively, suggesting that the greater the slope, the greater the maximum lateral pressure. However, lateral stress on the upper (0.5 H) and the lower (0.3 H) ground was found to increase as the slope was gradual. This represents the stress distribution in which the lateral stress on 0.3 H decreases with the gradual slope of the soilbag retaining wall, while the lateral stress on the upper and the lower parts of the soilbag retaining wall increases. In addition, the lateral earth pressure tends to be less than or equal to the static earth pressure, regardless of slope. The earth pressure by shaking table test was less than active earth pressure by Coulomb at the 0.2H point from the bottom, but greater than the active earth pressure by Coulomb at the (0.2~0.65) H point. It is also less than the active earth pressure by Coulomb beyond the 0.65 H point.

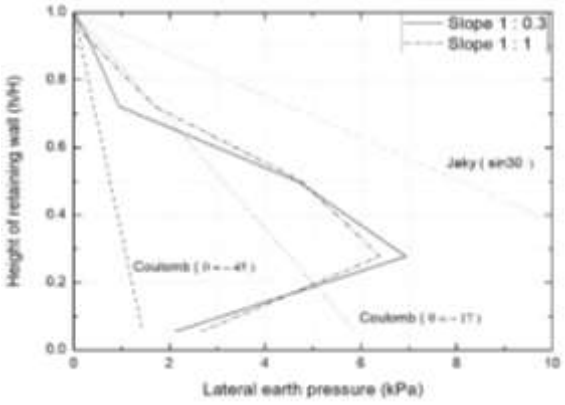

Fig. 10. Lateral earth pressure estimated by various methods and experimental work

Figs. 11 (a)~(d) provide the dynamic lateral earth pressure by the height of retaining wall and earthquake acceleration for soilbag retaining wall slope SB1-0.3. Figs. 11 (e)~(h) provide the dynamic lateral earth pressure per height of retaining wall for soilbag retaining wall slope SB1-1.0. Under all conditions, the dynamic earth pressure was found to be greater than that by the Mononobe-Okabe method for soilbag retaining wall slope SB1-1.0. Meanwhile, the dynamic earth pressure by the Mononobe-Okabe method was underestimated more than the result of the shaking table test for soilbag retaining wall slope SB1-0.3 and (0.154~0.22) g_n of earthquake acceleration. The underestimation of dynamic earth pressure by the Mononobe-Okabe method was caused by only the inertial force of backfilling ground at static equilibrium state, not of the wall that actually occurred in the shaking table test, being considered. Dynamic earth pressure at 0.33 g_n of earthquake acceleration tended to be similar to that by the Mononobe-Okabe method, but the dynamic earth pressure at 0.44 g_n of earthquake acceleration was greater than the result of the shaking table test.

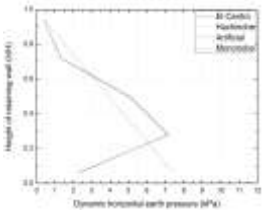
(a) 0.154 g_n (SB1-0.3)

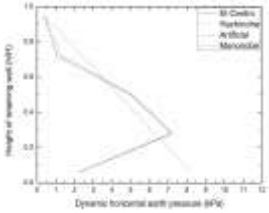
(b) 0.22 g_n (SB1-0.3)

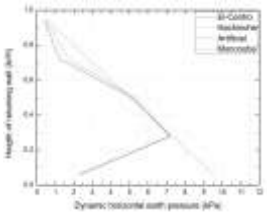
(c) 0.33 g_n (SB1-0.3)

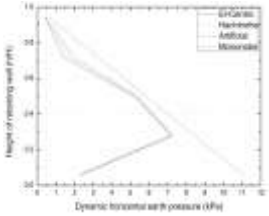
(d) 0.44 g_n (SB1-0.3)

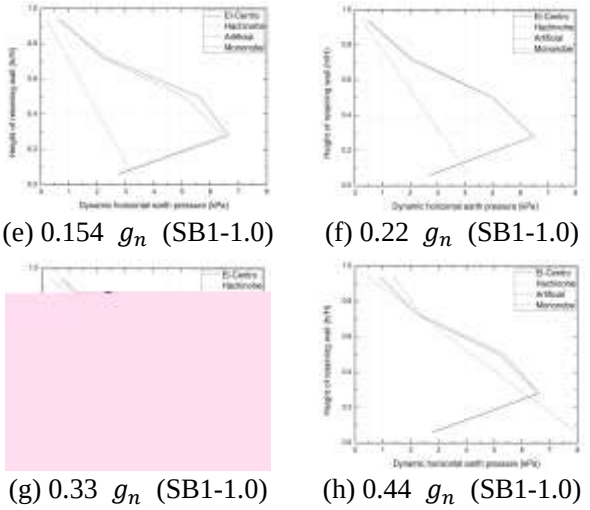

(e) 0.154 g_n (SB1-1.0) (f) 0.22 g_n (SB1-1.0)

(g) 0.33 g_n (SB1-1.0) (h) 0.44 g_n (SB1-1.0)

Fig. 11. Dynamic Lateral Earth Pressure by Earthquake Acceleration and Height of Retaining Wall.

Given that the Mononobe-Okabe method considers the inertial force of the backfilling ground at the static equilibrium state, dynamic active earth pressure (P_{ae}) is applied to 1/3H, as earth pressure on the retaining wall presents the triangular type of distribution. Sherif et al. (1982) and Mylonakis et al. (2007) reported by means of the shaking table test of 1 g_n that dynamic active earth pressure was applied at (0.42 and 0.33) H, respectively. Steedman and Zeng (1990) argued by the result of the dynamic centrifugal model experiment that the action point of the dynamic earth pressure on the retaining wall changed by acceleration, and was higher than 1/3 H. Seed and Whitman (1970) reported that only dynamic earth pressure was applied at 0.6 H of height. Ortiz et al. (1983) reported that the action point of earth pressure changed by acceleration, and was higher than 1/3 H. Atik and Sitar (2010) reported 1/3 H as the same as that at static state.

Fig. 12 show the dynamic active earth pressure and its increments upon earthquake that were calculated by using a graphic solution method. The result of analysis shows that the action point of dynamic active earth pressure was (0.378~0.396) H from the bottom at 1:0.3 of slope and (0.154~0.44) g_n of earthquake acceleration. The action point calculated as (0.401~0.418) H at 1:1 of slope implied that the action point tended rise as the slope decreased. The slope at the action point of dynamic active earth pressure on the soilbag retaining wall was found to be higher than the 0.33 H suggested by the Mononobe-Okabe method, because of not only the inertial force on the backfilling ground, but also that on the wall.

The increments of dynamic active earth pressure were determined at (0.493~0.538) H at 1:0.3 of slope and (0.154~0.44) g_n of earthquake acceleration and (0.610~0.630) H at 1:1 of slope, suggesting that increments tends to rise as the slope reduces. The action point of dynamic active earth pressure increments by the Seed and Whitman (1970) method was 0.6 H, which matches the theory of when the slope is gradual.

Relatively, the dynamic active earth pressure increments (ΔP_{ae}) are smaller than the active earth pressure at static state (P_a); therefore, the action point of dynamic active earth pressure (P_{ae}) is affected by active earth pressure. Accordingly, the action point of active earth pressure on the soilbag retaining wall at static state is high when the slope is gradual. The action point of dynamic active earth pressure upon earthquake is also high when the slope is gradual.

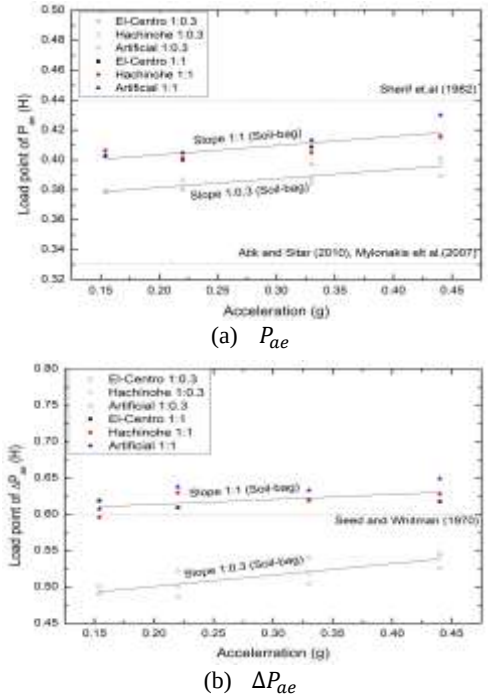

(a) P_{ae}

(b) ΔP_{ae}

Fig. 12. Action Point of Load.

5 CONCLUSION

Large-scale direct shear test, large-scale shaking table test were conducted to characterize the soilbag and connecting materials for analysis of dynamic load that occurred on the soilbag retaining wall system upon earthquake, and the following results were obtained.

The result of shaking table test applying (0.154~0.44) g_n of load based on 0.22 g_n of destruction-proof level in 2,400 of recurrence period showed that relative displacement occurred within the range of ±5 mm during the test, and almost no displacement occurred within 1 mm after the end of test. Even though the bounding effect of the shaking table wall that meets the < 300 mm of transverse displacement standard in Korea earthquake resistant design is considered. The soilbag retaining wall structure is determined as quite stable in terms of earthquake resistance.

Forces caused by dynamic earth pressure upon

earthquake to the backfilling ground and the soilbag retaining wall lead to phase difference, which is expressed as inertial force of wall. Due to such phase difference, the Mononobe-Okabe method with an assumption of static equilibrium state has the risk of underestimating dynamic earth pressure.

The slope of soilbag wall affects active earth pressure at the static state, and action point of increments of dynamic active earth pressure upon earthquake. As the slope is gradual, the action point of active earth pressure at the static state is high, and of increments of dynamic active earth pressure is low. Therefore, changing the range of action point of dynamic active earth pressure depending on the slope of soilbag retaining wall needs to be reflected in the design.

ACKNOWLEDGEMENTS

This research was supported by Korea Electric Power Corporation, 2017 (CX72166534).

REFERENCES

Anderson, D. G., Martin, G. R., Lam, I. P., and Wang, J. N. (2008), Seismic Design and Analysis of Retaining Walls, Buried Structures, Slopes and Embankments, NCHRP Report 611. Transportation Research Board, National Cooperative Highway Research Program, Washington, D. C.

Atik, L.A., Sitar, N. (2010), "Seismic Earth Pressures on Cantilever Retaining Structures", Journal of Geotechnical and Geoenvironmental Engineering, Vol. 136, No.10, pp.1324-1333.

Bolton, M.D., Steedman, R.S., (1982), "Centrifugal Testing of Microconcrete Retaining Walls subjected to Base Shaking" Proceedings of Conference on Soil Dynamics and Earthquake Engineering, Southampton, 1, pp.311-329

Chang, M. F. (1981), Static and Seismic Lateral Earth Pressures on Rigid Retaining Structures, Ph.D. Thesis, Purdue University West Lafayette, pp.466

Dubrova G. A. (1963), "Interaction of Soil and Structures", Rechoy Transport, Moscow, U.S.S.R

Elms, D. G., Richards, S. R. (1991), "Comparison of Limit State Seismic Earth Pressure Theories", Proceeding of 2nd International conference on Recent advances in Geotech Earthquake Engineering and Soil Dynamics, March 11-15, St. Louis, Missouri, No.4.9, pp.629-634

Jung, C., Bobet, A., and Femandez, G. (2010), "Analytical Solution of the Response of a Flexible Retaining Structure with an Elastic Backfill", Journal of Numerical and Analytical Methods in Geomechanics, Vol.34, pp.1387-1408

Kim, S. R., Kwon, O. S., and Kim, M. M., (2003), "Modeling of Force Components Acting on Quay Walls During Earthquakes", Journal of Korean Geotechnical Society, Vol.19, No.2, pp.107-121

Mononobe N., Matsuo O. (1929), "On the determination of earth pressure during earthquakes", Proceeding of the World Engineering Congress, vol. 9, Tokyo, Japan, pp. 179-187.

Richards, R., Elms, D. G. (1979), "Seismic Behaviour of Gravity Retaining Walls", Journal of Geotechnical Engineering, ASCE 105(GT4), pp.449-464.

Seed, H.B., and Whitman, R.V. (1970), "Design of earth retaining structures for dynamic loads" Proceedings of the Specialty Conference on Lateral Stresses in the Ground and Design of Earth Retaining Structures, ASCE. Cornell Univ., Ithaca, New York, pp.103-147

Sherif, M.A., Ishibashi, I., Lee, C.D. (1982), "Earth pressures against rigid retaining walls" Journal of Geotechnical Engineering, ASCE 108, pp. 679-695.

Yang C, Liu Z, Zhang J, Chen Z, Shi C, Gao H (2014) Analysis on mechanism of landslides under ground shaking: a typical landslide in the Wenchuan earthquake. Environ Earth Sci 72(9):3457–3466

Yang C, Zhang J, Wang Z, Cao L (2018) Research on time-frequency analysis method of active earth pressure of rigid retaining wall subjected to earthquake. Environ Earth Sci 77(6):1095‑1104